Effect of composition drift on emulsion copolymerization rate

G. H. J. van Doremaele, F. H. J. M. Geerts, H. A. S. Schoonbrood, J. Kurja and A. L. German*

Laboratory of Polymer Chemistry, Eindhoven University of Technology, PO Box 513, 5600 MB Eindhoven, The Netherlands

(Received 21 May 1991; accepted 25 June 1991)

With potassium persulphate as initiator and sodium dodecyl sulphate as emulsifier, the batch emulsion copolymerization rate behaviour of styrene (S) and methyl acrylate (MA) was investigated at 50°C, varying the monomer ratio and the monomer to water ratio. The composition drift occurring during the copolymerization is determined by the reactivity ratios and by the monomer partitioning between the various phases present in the emulsion system. Monomer partitioning studies show that the monomer ratio in the latex particles is equal to the monomer ratio in the droplets, although the total monomer swellability of the (co)polymer latex particles depends upon copolymer composition and monomer droplet composition. In the absence of monomer droplets the equilibrium monomer concentration in the aqueous phase is closer to its saturation value (i.e. water solubility) than the monomer concentration in the latex particles. As a consequence of the composition drift, the kinetic behaviour differs widely from the homopolymerizations depending upon the initial monomer ratio. The copolymerization rate strongly varies during copolymerization resulting in a conversion–time plot differing in shape from the sigmoidal shape usually observed in emulsion homopolymerization. The penultimate effect in S–MA copolymerization has been proved to be responsible for this, as can be seen clearly from the conversion dependence of the copolymerization rate during batch emulsion copolymerizations starting from an MA-rich monomer feed, leading to a strong composition drift.

(Keywords: emulsion copolymerization; composition drift; penultimate model; styrene; methyl acrylate)

INTRODUCTION

Batch (emulsion) copolymerization processes often produce highly heterogeneous copolymers with respect to chemical composition[1,2]. This heterogeneity may affect the product properties either beneficially or adversely. If required, this can be avoided by using more sophisticated processes such as semi-continuous (sometimes called semi-batch) processes[3–7] or controlled composition processes[8]. Before studying semi-continuous processes it is necessary to obtain a good knowledge of the conventional batch process.

Copolymerization rate is one of the important aspects of emulsion copolymerization, since it involves many complicated chemical and physical rate processes. Generally, the rate of emulsion polymerization strongly depends on temperature and the kind and amount of monomers, initiator and surfactants. A very important factor is the number of latex particles. The overall polymerization rate is proportional to the particle number, average number of radicals per particle and the monomer concentration inside the particles, the last being the main loci of polymerization. Normally, a conversion–time plot of an emulsion polymerization exhibits the well-known characteristic sigmoidal shape. Sometimes a sudden increase in polymerization rate at high conversion can be observed due to the gel effect. For instance, this effect was reported by Nomura *et al.* for styrene (S)–methyl methacrylate (MMA) emulsion copolymerization[9].

As compared with homopolymerizations, in copolymerizations the monomer feed ratio is an additional parameter significantly affecting copolymerization rate. This may result in an even more complex rate behaviour. Due to the occurrence of composition drift during emulsion copolymerization the conversion–time plot may exhibit different shapes. For the emulsion copolymerizations of vinyl acetate (VAc) with MMA[10], VAc with n-butyl acrylate (BA)[11,12] and VAc with methyl acrylate (MA)[13] it has been demonstrated that the conversion–time plots can exhibit a double bend. This was attributed to the fact that in these cases there is a large difference between the values of the reactivity ratios ($r_{VAc} < 0.1$ and $r_{(meth)acrylate} > 5$) in combination with a large difference between the propagation rate constants of the pertaining homopolymerizations. The large difference in reactivity ratios results in a strong composition drift. Vinyl acetate is polymerized in two stages. The first stage comprises a real copolymerization with the (meth)acrylate and during the second stage, after the (meth)acrylate has been depleted, a sudden increase in polymerization rate is observed and VAc practically homopolymerizes. According to the well-known ultimate model (Alfrey–Mayo kinetics) the average rate constant ($\bar{k}_p$) depends on the propagation rate constants of the homopolymerizations and is also a function of the reactivity ratios

* To whom correspondence should be addressed

0032-3861/92/091914-08

and the (local) monomer feed ratio. In these systems the (average) $\bar{k}_p$ strongly depends upon the monomer ratio, because the k_ps of the homopolymerizations are very different.

The aim of the current investigation is to furnish further fundamental information about the kinetic mechanism of S–MA emulsion copolymerization. It might be expected that the emulsion copolymerization of S and MA exhibits a similar kind of kinetic behaviour as VAc–BA, because the reactivity (k_p) of MA is high as compared with that of S and the values of the reactivity ratios in combination with the higher water solubility of MA result in a significant composition drift. Moreover, Davis *et al.*[14] recently found a penultimate effect for the copolymerizations of S–MA and S–BA, where k_p is strongly dependent on monomer ratio. Ramirez-Marquez *et al.*[15,16] investigated the effect of initiator concentration, emulsifier concentration and monomer to water ratio on the (co)polymerization rate of S–MA emulsion copolymerization. Although they observed the occurrence of a strong composition drift in MA-rich recipes, from their limited conversion–time data they did not notice a sudden increase in polymerization rate at the moment S is almost totally depleted. As a result they were able to describe the S–MA emulsion copolymerization rate by means of the ultimate model. This obligated us to perform very accurate kinetic measurements in order to investigate whether the occurrence of composition drift would affect the average propagation rate constant and whether this phenomenon is reflected in the conversion–time curves.

In order to accurately describe emulsion copolymerization by means of a model, it is of paramount importance to implement a reliable description of the monomer concentrations within the latex particles. The monomers are distributed between the particles, the aqueous phase and, if present, the monomer droplets. In emulsion (co)polymerization it is generally recognized that the monomer partitioning is determined by thermodynamic equilibrium. Equilibrium requires the chemical potential of the monomers to be equal in all phases present. Morton *et al.*[17] developed a model that describes the monomer partitioning in the case of one monomer. This model is based on the classical Flory–Huggins lattice theory for monomer–(homo)polymer mixtures and includes an interfacial energy term. Morton stated that even in those cases where the monomer is a good solvent for the polymer only a limited amount of monomer is absorbed by the latex particles, because the increase of surface energy on swelling compensates for the free energy gain of mixing.

Guillot[18] extended the thermodynamic monomer partitioning treatment of Morton, in an effort to describe the monomer partitioning during emulsion *co*polymerization by introducing interaction terms for the monomers. Guillot gave equations to calculate the monomer and polymer volume fractions and (partial molar) free energies of both monomers in the three phases.

In the last few years the thermodynamic treatment has been applied by several investigators[19–23]. However, at present no reliable method of predicting the free energy of a monomer swollen latex particle is available. The use of models to describe the very complicated phenomena of monomer partitioning and also the lack of sufficient and accurate experimental monomer partitioning data frequently results in unreliable or unrealistic estimations of interaction parameters.

Among all emulsion copolymerization systems the monomer partitioning behaviour of S–MMA has been most extensively described. Nomura[10] performed numerous monomer equilibrium experiments on S–MMA, determining the effect of monomer ratio, particle size, copolymer composition, interfacial tension and ionic strength on the latex particle swellability. For other copolymer systems such detailed data are not available.

The above considerations provided sufficient motives to perform a set of equilibrium experiments to study the effect of several parameters (monomer ratio, copolymer composition and molecular mass, crosslink density and particle size) on the monomer partitioning in S–MA emulsion copolymerization systems. Experiments were carried out with or without the presence of a separate monomer layer. The experiments with a monomer layer are representative for intervals I and II of the emulsion copolymerization, whereas the experiments without a separate monomer layer are representative for interval III of the emulsion copolymerization.

EXPERIMENTAL

Equilibrium monomer partitioning experiments

A latex of known solid content (determined by means of standard dry solid content analysis) and copolymer composition was mixed with known amounts of the two monomers in the absence of initiator. Prior to use the latex had been heated (90°C) for 24 h in order to remove the last traces of the initiator. The system was allowed to reach equilibrium by shaking (for at least 24 h) while thermostatically controlled at the chosen temperature. The phases (swollen polymer particles, aqueous phase and monomer layer) were separated using an ultracentrifuge (380 000*g*, Centrikon, T-2060, 1–3 h) thermostatically controlled at a maximum temperature of 45°C. The swollen particles could not be analysed without including a small part of the adhering aqueous phase. Monomer concentrations in the particle phase were determined by means of gas–liquid chromatography (g.l.c.) after dissolving the monomer swollen (co)polymer phase (with minor aqueous phase content) in acetone with toluene as an internal standard or, alternatively in the case of polystyrene (PS) latices, after dissolving in toluene with 2-propanol (IPA) as internal standard. Determination of dry solid content of the sample gave the copolymer content. The concentration of MA in the aqueous phase was determined after adding a standard IPA solution in water to the aqueous layer. The presence of styrene (<3 mmol l^{-1}) in the water phase was neglected. For the determination of the monomer concentrations in the particles, appropriate corrections were performed for the MA content in the sample, dissolved in the aqueous phase. If present, the monomer layer was analysed by means of g.l.c. in terms of molar monomer ratio. This monomer ratio was always in very good agreement with the value calculated from the mass balance equations. To calculate the monomer concentrations inside the particles, the volumes of all components (monomers and (co)polymer) present in the monomer swollen latex particles were assumed to be additive. Copolymer density was calculated by the appropriate averaging of the densities of the homopolymers (*Table 1*).

The reliability of the method mentioned above was confirmed by means of additional monomer equilibrium

Table 1 Densities of monomers and polymers used

Monomer	Density ($g\ cm^{-3}$)	Temperature (°C)
Styrene	0.9060	20
Methyl acrylate	0.9535	20
Polystyrene	1.05	20
Poly(methyl acrylate)	1.2	20

experiments (without a separate monomer phase present) using common dialysis tubing for the separation of the aqueous phase serum from the latex particles. Phase equilibrium was always achieved within 30 min.

Emulsion copolymerizations

The emulsion copolymerizations were carried out under nitrogen in a 1 l glass or 1.3 l stainless-steel vessel normally thermostatically controlled at 323 K. The principle of on-line g.l.c. analysis has been described by Rios *et al.*[24] and German and Heikens[25]. Alternatively, it would have been possible to use head-space analysis[26]. We have chosen the following modification. The reaction mixture is pumped in a sample loop using a pulsating membrane pump (Orlita, type TW 1515/MK00). In order to prevent phase separation the reaction mixture is circulated continuously throughout the entire course of the emulsion polymerization. Up to 33 wt% latices could be pumped without pump or sampling valve fouling which would cause analysis problems. By means of the sampling valve[25] present in the sample loop, a constant volume of reaction mixture can be analysed at any time during reaction. As a consequence of the heterogeneity of the emulsion, relatively large sample volumes had to be taken (5 μl). This 'large' sample appeared to be representative of the heterogeneous emulsion polymerization system as a whole and gave significantly less scatter of g.l.c. data, as compared with a smaller sample volume (for instance 1 μl). Normally, the scatter of peak areas of each monomer, due to variations in sample volume and due to the heterogeneity of the emulsion, was $<20\%$ during intervals I and II of the emulsion (co)polymerization and $<10\%$ during interval III. No internal standard was used in order not to influence copolymerization behaviour in this heterogeneous system. The scatter of the *ratio* of peak areas of both monomers was $<5\%$ during the entire course of the reaction.

The monomers and the water present in the sample mixture are evaporated in an injection block (placed directly after the sample chamber) thermostatically controlled at $\sim$473 K, and as a result the copolymer present in the sample is retained. The gas phase is subsequently split at a variable ratio (but fixed within each single experiment) in order to prevent overloading of the column (HP-1 methyl silicone gum wide-bore column (length × internal diameter × film thickness = 5 m × 0.53 mm × 2.65 μm, thermostatically controlled at 378 K) and overloading of the detector (flame ionization detector, 473 K). The g.l.c. was carried out using a Carlo-Erba Instruments GC 6000 Vega series 2. Helium was used as carrier gas. A personal computer (Atari 1040 ST) operated the pneumatic sampling valve, integrated the chromatograms and calculated partial conversions of both monomers. Usually, every 2 min a sample was taken for g.l.c. analysis. Reactions were commonly followed during 4 h, thus 120 samples were taken, in addition to the 10 or 20 g.l.c. reference samples taken prior to polymerization. The amount of copolymer residue that remained in the injection block generally did not cause any problems to sample and carrier gas passage, provided no more than 120 samples were taken during reaction. At the end of every experiment the sample valve and injection block were disconnected and cleaned. No fouling inside the sample chamber was ever observed. This may be attributed to the continuous circulation of the reaction mixture.

Before use the reactor was purged with nitrogen in order to remove oxygen. The monomers, in which n-dodecyl mercaptan (NDM) was dissolved, were added dropwise to the sodium dodecyl sulphate (SDS) solution in water. The emulsion was stirred with a 12-bladed turbine stirrer at 250 rev min^{-1}. After the emulsion had reached reaction temperature and the reference g.l.c. determinations were performed, the reaction was started by adding a potassium persulphate ($K_2S_2O_8$) solution in water to the reaction mixture. No induction time was observed.

The overall ratio of monomers during the entire course of the reaction was monitored by means of on-line g.l.c. Total weight conversion was determined by means of dry solid analysis. Polymerization in the dry solid samples was stopped by adding hydroquinone (Merck). After curve fitting of the g.l.c. data, partial conversions of both monomers were calculated combining both data sets.

The polymerizations were carried out with a SDS concentration of 0.0116 mol l^{-1} and with a $K_2S_2O_8$ concentration of 1.233 mmol l^{-1}. The monomer ratio, the monomer to water ratio, and the NDM concentration (usually 1 wt% on monomer basis) were varied. $NaHCO_3$ was added (1.223 mmol l^{-1}) maintaining a sufficient pH level. Particle size measurements were performed with TEM after u.v. hardening of the latex and by means of dynamic light scattering (d.l.s.).

The size of the monomer droplets under the experimental conditions was measured applying a method described by Hoedemakers[27]. The volume-mean diameter of the monomer droplets was $\sim$15 μm. As is generally recognized, in this range of monomer droplet sizes there is no significant diffusion limitation of monomer transport from the droplets to the aqueous phase. Furthermore, polymerization inside the monomer droplets is negligible.

RESULTS

Monomer partitioning

Methyl acrylate concentration in the aqueous phase as a function of composition of monomer phase, and SDS concentration. In the presence of a separate monomer phase the aqueous phase concentration of S is always <3 mmol l^{-1} and can be neglected in the emulsion copolymerization model calculations. The concentration of MA in the aqueous phase linearly increases when the mole fraction of MA in the monomer phase increases (*Figure 1*). The partitioning coefficient K_{MA} ($=[MA]_w/[MA]_d$) is $\sim$0.05. As already pointed out by Emelie *et al.*[28] for BA and MMA the type and concentration of surfactants can affect the water solubility of a monomer. Above the critical micelle concentration ($\sim$2.2 $g^{-1}\ l^{-1}$ for SDS) this effect is reinforced by the monomer solubilization within micelles. In *Figure 2* it is demonstrated, however, that the effect of SDS concentration ($<4\ g\ l^{-1}$) on the water solubility of MA is negligible.

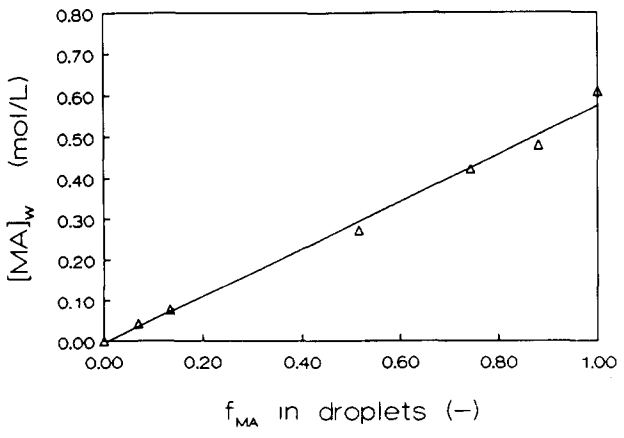

Figure 1 MA concentration in the aqueous phase as a function of monomer phase composition at 50°C

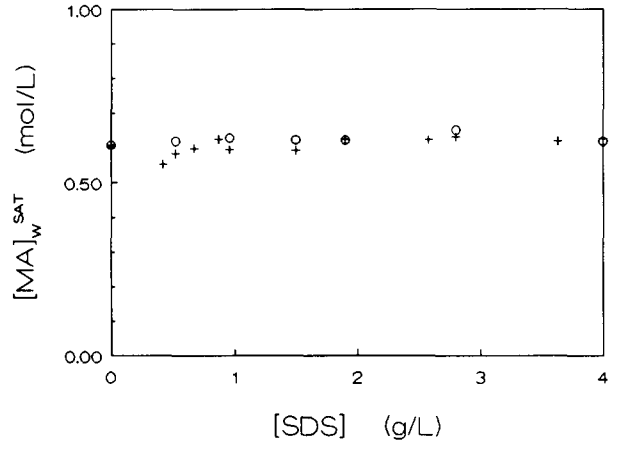

Figure 2 Water solubility of MA depending upon SDS concentration and temperature: (○) 45°C; (+) 50°C

Methyl acrylate partitioning between aqueous phase and polymer particles in the absence of a separate monomer phase. During S–MA batch emulsion copolymerization, especially in the case of the very interesting MA-rich recipes, at moderate total conversion the major part of the S has already been depleted while a major part of the MA is still present. Therefore, the MA concentration inside the particles ($[MA]_p$) *versus* the MA concentration in the aqueous phase ($[MA]_w$) was determined in the absence of S. All these experiments were carried out at 45°C. In *Figure 3a* it is demonstrated that in the absence of a separate monomer phase, $[MA]_w$ is closer to the saturation value (i.e. water solubility) than $[MA]_p$ in poly(methyl acrylate) (PMA) latex particles (i.e. $[MA]_w/[MA]_w^{sat} > [MA]_p/[MA]_p^{sat}$). This swelling behaviour of MA is similar to that of S in PS particles and MMA in poly(methyl methacrylate) particles[29]. Furthermore, it is shown that the presence of crosslinks in the PMA particle on the swellability is negligible. Apparently, the extent of crosslinking is too low to restrict the monomer swelling of the latex particles. The crosslinked PMA latex was prepared in the presence of 5 mol% ethylene diacrylate.

In *Figures 3b, c* and *d* the effect of copolymer composition (of S–MA (co)polymer), particle size and molar mass on MA partitioning is shown. At MA concentrations close to saturation a very small influence

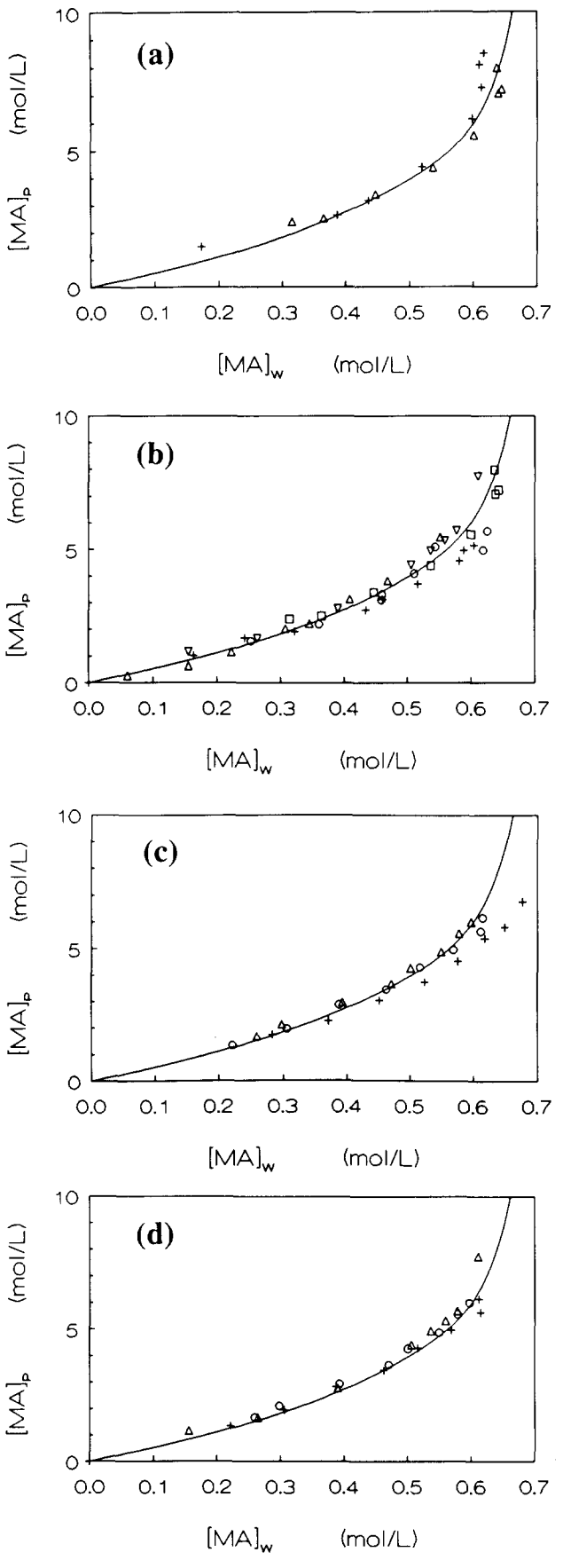

Figure 3 MA concentration in the particles as a function of MA concentration in the aqueous phase. Lines are calculated according to equation (4). (a) PMA latex particles; (+) crosslinked and non-crosslinked (△) PMA. (b) Effect of copolymer composition; F_S = (□) 0, (▽) 0.25, (○) 0.5, (△) 0.75 and (+) 1. (c) Effect of particle size ($F_S = 0.25$); D_w (nm) = (+) 32, (○) 61 and (△) 97. (d) Effect of copolymers molar mass ($F_S = 0.25$); M_w (g mol^{-1}) = (○) 7500, (△) 48 000 and (+) 1 300 000

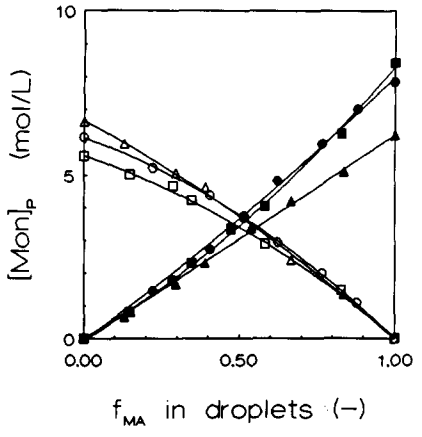

Figure 4 Monomer (S and MA) concentrations inside the latex particles as a function of the composition of the monomer phase: (▲) $[MA]_p$, PS; (●) $[MA]_p$, PS–MA (with $F_S = 0.5$); (■) $[MA]_p$, PMA; (△) $[S]_p$, PS; (○) $[S]_p$, PS–MA (with $F_S = 0.5$); (□) $[S]_p$, PMA

is noticed. This effect, however, is negligible in practical simulations. Lower molar mass, larger MA content in the (co)polymer and larger particle size increase the equilibrium $[MA]_p$ as a function of $[MA]_w$. Combining all data of *Figure 3*, $[MA]_p$ can be expressed as a function of $[MA]_w$ by the empirical fitting equation:

$$[MA]_p = 5.1[MA]_w + 11.0[MA]_w^3 + ([MA]_w + (1 - [MA]_w^{sat}))^y \quad (1)$$

where $y = 30$.

Monomer partitioning in the presence of a separate monomer phase. In *Figure 4* the monomer concentrations inside the particles (in moles of monomer per litre of swollen latex particle volume) are given, with (co)-polymer composition as parameter, as a function of the composition of the monomer phase (20°C). The lines represent second-order polynomials obtained by linear least square fitting of the data. For comparison, the concentrations of the pure monomers are: S 8.7 mol l^{-1} and MA 11.1 mol l^{-1}. In *Figure 5* the monomer composition in the particles is compared with the monomer composition of the monomer phase.

From *Figure 4* it is concluded that the monomer swellability of polymer particles increases with increasing MA content. The monomer ratio in the droplets is equal to the monomer ratio in the swollen particles for all monomer ratios and all copolymer chemical compositions studied (*Figure 5*). Copolymer composition only affects the total monomer concentration inside the latex particles. The curves of the monomer concentrations in the particles *versus* the mole fraction of the same monomer in the monomer phase are curved in such a manner that, independent of the monomer ratio in the monomer phase (droplets), the monomer ratio in the particles is equal to the monomer ratio in the monomer phase, although the total monomer concentration may still depend on the monomer ratio in the monomer phase. Nomura and Fujita found a similar behaviour for S–MMA[10].

It is known that solution copolymerizations of monomers strongly differing in polarity (e.g. S and acrylic acid) only can be described by 'apparent' reactivity ratios that depend on the solvent used. This can be explained by the 'bootstrap' model, presented by Harwood[30], that accounts for local monomer concentrations in the environment of the growing radical chains differing from the overall monomer concentrations. The result of *Figure 5* (monomer ratio independent of the composition of the (co)polymer present) suggests the absence of a 'bootstrap' effect. This is in agreement with the findings that reactivity ratios of these systems are only weakly dependent on solvent[31]. Similar monomer partitioning behaviour has also been found for the MA–BA and S–BA systems[32].

Copolymerization rate behaviour

A typical conversion–time curve of a batch emulsion copolymerization of S with MA is given in *Figure 6a*. The initial monomer ratio $(S/MA)_0$ was 0.33 mol mol^{-1} with a monomer to water ratio $(M/W)_0$ of 0.2 g g^{-1}. From this plot it is obvious that the S–MA copolymerization passes through several stages. Polymerization starts with the particle nucleation stage. After 10% conversion an almost constant copolymerization rate is observed until 40% conversion. Copolymerization rate then decreases between 40% and 55% conversion. This decrease in copolymerization rate is attributed to a decrease in monomer concentrations in the latex particles. At the point at which S is (almost) totally depleted, the polymerization rate is at a minimum. From this point on the reaction rate suddenly increases MA homopolymerizes. Depletion of MA, the preferential presence of MA in the aqueous phase, and diffusion controlled propagation, result in a final decrease of polymerization rate at high conversions. This indicates that composition drift strongly affects the S–MA copolymerization rate.

In order to obtain further insight in the underlying mechanisms that control the sudden acceleration of the polymerization rate, the $(S/MA)_0$ (*Figure 7*) and $(M/W)_0$ (*Figure 8*) have been changed. All experiments with a S content of $< 50\%$ were found to exhibit a sudden increase in polymerization rate at the moment where S has almost totally been consumed. No sudden increase in polymerization rate was noticed in the case of higher S contents. As has already been noted by Ramirez-Marquez and Guillot[15], higher MA fractions in the initial monomer feed result in a higher polymerization rate.

As depicted in *Figure 7* at lower $(S/MA)_0$ ratios acceleration and pure PMA formation occurs at a lower conversion. As depicted in *Figure 8* a decrease of

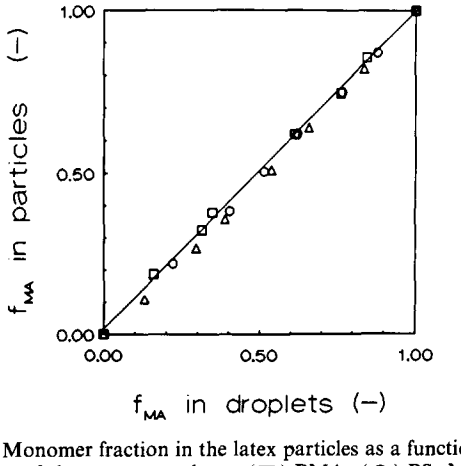

Figure 5 Monomer fraction in the latex particles as a function of the composition of the monomer phase: (□) PMA; (○) PS–MA (with $F_S = 0.5$); (△) PS

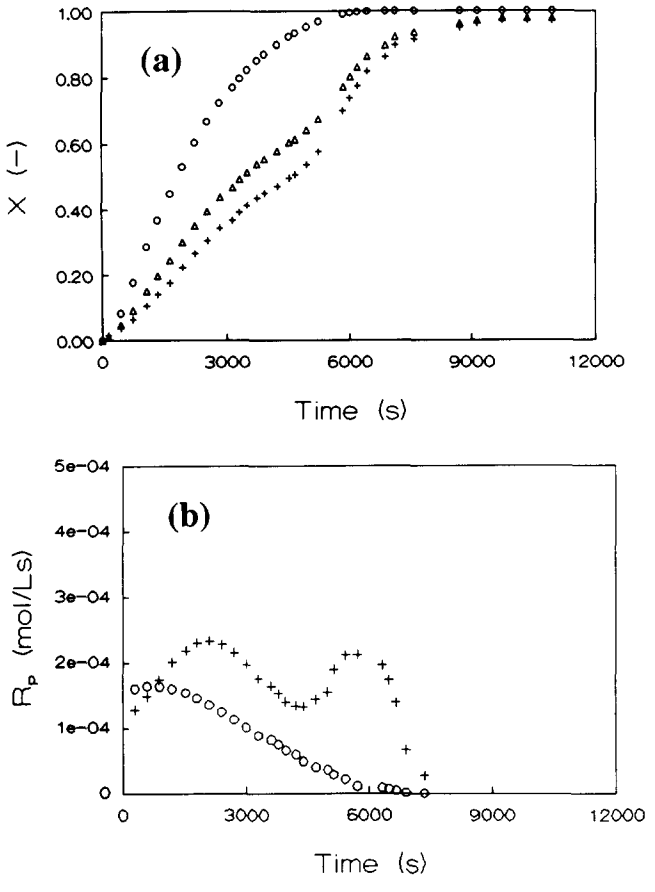

Figure 6 Batch emulsion S–MA copolymerization at 50°C with $(S/MA)_0 = 0.33$ mol mol^{-1}, $(M/W)_0 = 0.2$ g g^{-1}, SDS concentration = 0.0116 mol l^{-1}, $K_2S_2O_8$ concentration = 1.233 mmol l^{-1}, $NaHCO_3$ concentration = 1.233 mmol l^{-1} and 1 wt% NDM. (a) Conversion–time plot: (+) MA conversion; (○) S conversion; (△) total mole conversion. (b) Polymerization rate–time plot: (+) MA; (○) S

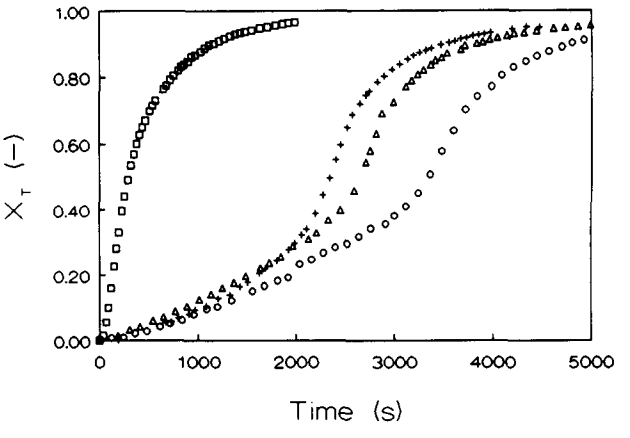

Figure 7 Conversion–time plots of batch emulsion S–MA copolymerizations at 50°C with $(M/W)_0 = 0.2$ g g^{-1}, SDS concentration = 0.0116 mol l^{-1}, $K_2S_2O_8$ concentration = 1.233 mmol l^{-1}, $NaHCO_3$ concentration = 1.233 mmol l^{-1}, 1 wt% NDM and a variable monomer feed ratio: $(S/MA)_0$ (mol mol^{-1}) = (□) 0, (+) 1/19, (△) 1/11, (○) 1/7

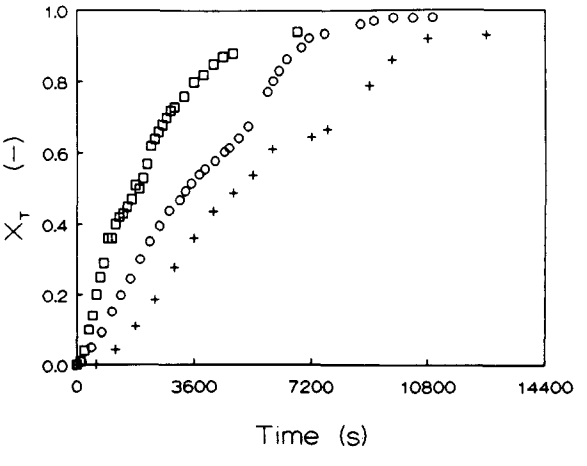

Figure 8 Conversion–time plots of batch emulsion S–MA copolymerizations at 50°C with $(S/MA)_0 = 0.33$ mol mol^{-1}, SDS concentration = 0.0116 mol l^{-1}, $K_2S_2O_8$ concentration = 1.233 mmol l^{-1}, $NaHCO_3$ concentration = 1.233 mmol l^{-1}, 1 wt% NDM and variable initial monomer to water ratios: $(M/W)_0$ (g g^{-1}) = (□) 0.05, (○) 0.2, (+) 0.5

monomer to water ratio results in a higher fractional (co)polymerization rate. Because of the stronger composition drift due to the buffer capacity of water for MA, this also results in a lower critical conversion at which the acceleration of polymerization rate occurs (*Figure 9*).

From these experiments it can be concluded that composition drift is an important factor determining copolymerization rate behaviour. In principle this behaviour could be attributed to several possible mechanisms, since the polymerization rate is proportional to: (a) the number of latex particles; (b) the monomer concentration inside the particles; (c) the number of radicals per particle (influenced by a gel effect); and (d) the average propagation rate constant.

Mechanism (a). The acceleration observed could be attributed to a sudden increase in particle number (secondary nucleation) at the moment at which the homopolymerization of the more water soluble monomer (in this case MA) starts. More water soluble (hydrophilic) monomers have the tendency to form more latex particles in emulsion polymerization as compared with less water soluble monomers. However, d.l.s. measurements and transmission electron micrographs (after u.v. hardening of the latex) did not indicate a significant amount of small PMA particles at high conversion (*Figure 10*). Only a very small, gradual increase in particle number was

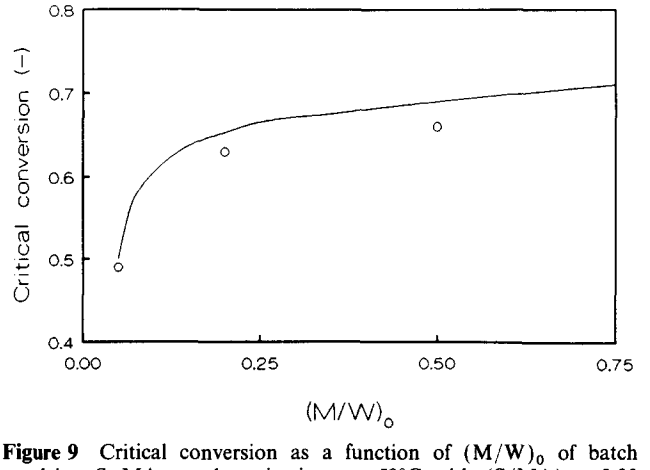

Figure 9 Critical conversion as a function of $(M/W)_0$ of batch emulsion S–MA copolymerizations at 50°C with $(S/MA)_0 = 0.33$ mol mol^{-1}, SDS concentration = 0.0116 mol l^{-1}, $NaHCO_3$ concentration = 1.233 mmol l^{-1}, 1 wt% NDM and $K_2S_2O_8$ concentration = 1.233 mmol l^{-1}. The line represents the model calculation

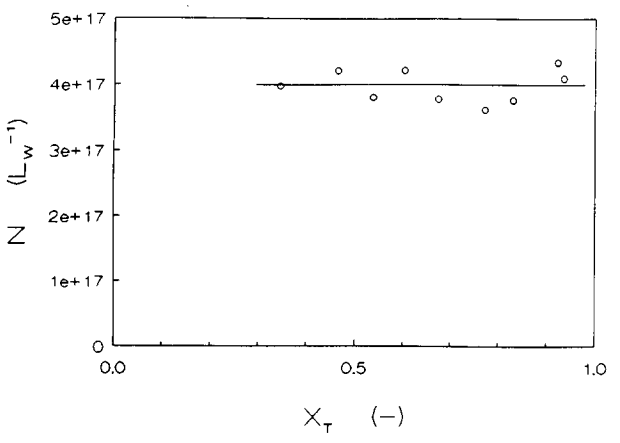

Figure 10 Particle number calculated from d.l.s. data *versus* conversion of a S–MA batch emulsion copolymerization at 50°C: $(S/MA)_0 = 0.33$ mol mol^{-1}, $(M/W)_0 = 0.2$ g g^{-1}, SDS concentration = 0.0116 mol l^{-1}, $NaHCO_3$ concentration = 1.233 mmol l^{-1}, 1 wt% NDM and $K_2S_2O_8$ concentration = 1.233 mmol l^{-1}

sometimes observed[15]. The final latex particles appeared to exhibit a core–shell type of morphology, as can be explained by the composition drift and the incompatibility of the (co)polymers formed. Furthermore, a significant increase in latex particle number is unlikely to occur, since the monomer droplets already disappeared below 50% conversion and, as a consequence, at 50% conversion the major part of the unreacted monomer MA is already inside the latex particles. Only a small part of the MA (<0.6 mol l^{-1}) is dissolved in the aqueous phase.

Mechanism (*b*). During interval III of the emulsion polymerization an increase in (average) $[MA]_p$ is of course impossible. However, an increase in local MA concentration in the shells of the polymer particles cannot be completely ruled out. The equilibrium concentration of MA is higher in PMA latex particles than in PS latex particles, 8.5 and 6 mol l^{-1}, respectively. Given these data, however, this phenomenon cannot be a major factor causing the sudden strong increase in rate. Therefore, a possible monomer concentration gradient inside the particles, due to differences between the thermodynamic interactions of MA with PMA and MA with copolymer (PS–MA), could only be slightly responsible for the observed increase in polymerization rate.

Mechanism (*c*). At first sight the gel effect, causing an increase of the average number of radicals per particle ($\bar{n}$), might cause the observed acceleration. MA is well-known for its gel effect. However, for several reasons the gel effect must be ruled out as a main cause in suddenly increasing the polymerization rate, although it will probably affect the rate to some extent. This is because, when varying initial monomer ratios, the increase in polymerization rate was found to occur at different conversions, and thus at different monomer concentrations, different volume fractions and different chemical compositions of the copolymer in the monomer swollen latex particles (*Table 2*). Invariably, in all cases the increase in rate was found to occur just at the moment S was exhausted.

Moreover, it was found that the presence and the amount (ranging from 0 to 10 wt% on monomer basis) of NDM, having a paramount effect on molar mass of the copolymer formed, did not affect polymerization rate. As a consequence, the occurrence of an important gel effect can be ruled out, because, as reported by Matheson *et al.*[33], the gel effect occurring during bulk polymerization of MA is eliminated by the presence of a small amount of chain transfer agent.

The average number of radicals inside latex particles was calculated at any moment from polymerization rate data, the $\bar{k}_p$ (*Figure 11*), the monomer concentrations inside the latex particles and the number of latex particles. For the experiment given in *Figure 6* the calculated values of $\bar{n}$ were ~0.3. However, due to errors and uncertainties in all parameters the values of $\bar{n}$ must be regarded as an approximation and not as absolute values, and therefore should be prudently used.

Mechanism (*d*). The cause of the sudden increase in rate may also be found in $\bar{k}_p$. The composition and sequence distribution of the copolymer formed and the composition drift during a copolymerization of S and MA can be adequately described by the ultimate model[34]. However, recent measurements of $\bar{k}_p$ as a function of monomer ratio by Davis *et al.*[14] using the laser-flash technique (comparable to the well-known rotating sector method) in low-conversion bulk and solution systems revealed that the kinetic behaviour of the S–MA system cannot be adequately described by the ultimate model. Instead the penultimate model proved to be

Table 2 Initial overall monomer ratio $(S/MA)_0$ and composition ($f_{m,0}$) of various batch emulsion copolymerizations, together with the critical mole fraction of the monomer inside the swollen latex particles ($f^c_{m,1}$), the critical volume fraction of polymer (v^c_p) in the swollen latex particles and the critical copolymer composition (F^c_m) at which acceleration occurs

$(S/MA)_0$	$f_{m,0}$	$f^c_{m,1}$	v^c_p	F^c_m
1/3	0.75	0.93	0.74	0.62
1/7	0.88	0.99	0.53	0.72
1/11	0.92	0.98	0.38	0.75
1/19	0.95	0.97	0.26	0.81

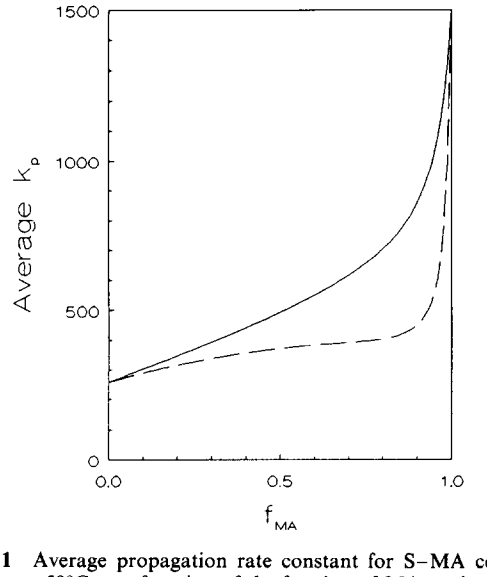

Figure 11 Average propagation rate constant for S–MA copolymerizations at 50°C as a function of the fraction of MA at the locus of reaction calculated according to the ultimate model (——) and the penultimate model (– – –)[14]

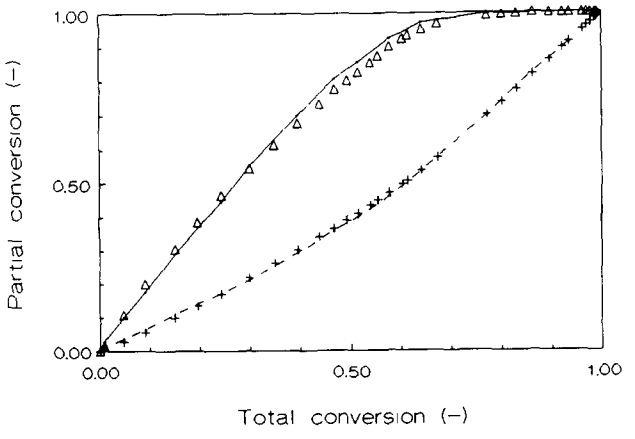

Figure 12 Experimental data of partial conversions of S (△) and MA (+) *versus* overall mole conversion compared to model calculations of an emulsion copolymerization with $(S/MA)_0 = 0.33$ mol mol^{-1} and $(M/W)_0 = 0.2$ g g^{-1}

appropriate in this case. Given the fact that composition drift is well described by the ultimate model, it can easily be demonstrated that from the six reactivity ratios in the penultimate model, two pairs of reactivity ratios are equal. Given the homopropagation rate constants of MA[14] being >3400, and of S[35] being 258 l mol^{-1} s^{-1} at 50°C, $\bar{k}_p$ can be calculated from the reactivity ratios, ($r_S = r'_S = 0.73$, $r_{MA} = r'_{MA} = 0.19$, $s_S = 0.94$ and $s_{MA} = 0.11$; $s_i = k_{jii}/k_{iii}$).

In *Figure 11* values of k_p have been plotted *versus* MA mole fraction in the local monomer feed, according to the ultimate model (inadequate in this case) and the penultimate model (adequate after recent findings). As can be seen from *Figure 11*, $\bar{k}_p$ strongly increases going from a monomer feed with 10% S to pure MA. Thus the sudden increase in polymerization rate can be attributed to the penultimate effect of the copolymerization of S and MA.

In *Figure 12* the experimentally determined partial conversions *versus* total conversion are compared with a model calculation[32]. From the satisfying agreement it can be concluded that, using independently determined monomer partitioning data and reactivity ratios, the model also correctly predicts the critical conversion at which the sudden acceleration occurs (*Figure 9*).

CONCLUSIONS

In the acrylate-rich batch emulsion copolymerizations of S with MA a strong composition drift is observed. The composition drift is determined by the reactivity ratios and the monomer partitioning.

From the equilibrium monomer partitioning experiments in the absence of a separate monomer layer it can be concluded that the MA concentration in the aqueous phase is closer to the saturation value than the MA concentration in the latex particles. The monomer partitioning in the systems investigated is only marginally affected by particle size, copolymer composition and molar mass.

The monomer partitioning experiments in the presence of a separate monomer layer revealed that the monomer ratio in the particles is equal to the monomer ratio in the monomer droplets, although the total monomer concentration in the swollen latex particles depends upon copolymer composition and upon monomer ratio in the droplets.

The occurrence of a penultimate effect in the propagation rate is reflected in the emulsion copolymerization conversion–time curve by a sudden increase in polymerization rate at the moment all S is depleted. The critical conversion at which the acceleration occurs can be predicted by a model by taking into account the reactivity ratios and the monomer partitioning, the latter depending upon initial monomer ratio and monomer to water ratio.

REFERENCES

1 van Doremaele, G. H. J., van Herk, A. M. and German, A. L. *Makromol. Chem., Macromol. Symp.* 1990, **35/36**, 231
2 Guillot, J. *Makromol. Chem., Macromol. Symp.* 1990, **35/36**, 269
3 El-Aasser, M. S., Makgawinata, T., Vanderhoff, J. W. and Pichot, C. *J. Polym. Sci., Polym. Chem. Edn.* 1983, **21**, 2363
4 Misra, S. C., Pichot, C., El-Aasser, M. S. and Vanderhoff, J. W. *J. Polym. Sci., Polym. Chem. Edn.* 1983, **21**, 2383
5 Garcia-Rejon, A., Guzman, C., Mendez, J. C. and Rios, L. *Chem. Eng. Commun.* 1983, **24**, 71
6 Arzamendi, G. and Asua, J. M. *J. Appl. Polym. Sci.* 1989, **38**, 2019
7 Arzamendi, G. and Asua, J. M. *Makromol. Chem., Macromol. Symp.* 1990, **35/36**, 249
8 Guyot, A., Guillot, J., Pichot, C. and Rios-Guerrero, L. *Am. Chem. Soc. Symp. Ser.* 1981, **165**, 415
9 Nomura, M., Horie, I., Kubo, M. and Fujita, K. *J. Appl. Polym. Sci.* 1989, **37**, 1029
10 Nomura, M. and Fujita, K. *Makromol. Chem., Suppl.* 1985, **10/11**, 25
11 Kong, X. Z., Pichot, C. and Guillot, J. *Eur. Polym. J.* 1988, **24**, 485
12 Delgado, J., El-Aasser, M. S., Silebi, C. A. and Vanderhoff, J. W. *J. Polym. Sci., Polym. Chem. Edn.* 1990, **28**, 777
13 Leiza, J. personal communication, 1989
14 Davis, T. P. personal communication, 1990
15 Ramirez-Marquez, W. and Guillot, J. *Makromol. Chem.* 1988, **189**, 361
16 Ramirez-Marquez, W. and Guillot, J. *Makromol. Chem.* 1988, **189**, 379
17 Morton, M., Kaizerman, S. and Altier, M. W. *J. Colloid Sci.* 1954, **9**, 300
18 Guillot, J. *Acta Polym.* 1981, **32**, 593
19 Mead, R. N. and Poehlein, G. W. *Ind. Eng. Chem. Res.* 1988, **27**, 2283
20 Mead, R. N. and Poehlein, G. W. *Ind. Eng. Chem. Res.* 1989, **28**, 51
21 Maxwell, I. A., Kurja, J., van Doremaele, G. H. J. and German, A. L. *Makromol. Chem.* in press
22 Forcada, J. and Asua, J. M. *J. Polym. Sci., Polym. Chem. Edn.* 1990, **28**, 987
23 Dimitratos, J., Georgakis, C., El-Aasser, M. S. and Klein, A. *Comp. Chem. Eng.* 1989, **13**, 21
24 Rios, L., Pichot, C. and Guillot, J. *Makromol. Chem.* 1980, **181**, 677
25 German, A. L. and Heikens, D. *J. Polym. Sci. A1*, 1971, **9**, 2225
26 Alonso, M., Alivers, M., Puigjaner, L. and Recasens, F. *Ind. Eng. Chem. Res.* 1987, **26**, 65
27 Hoedemakers, G. F. M. *PhD Thesis* Eindhoven University of Technology, 1990
28 Emelie, B., Pichot, C. and Guillot, J. *Makromol. Chem., Suppl.* 1985, **10/11**, 43
29 Gardon, J. L. *J. Polym. Sci. A1*, 1968, **6**, 2859
30 Harwood, H. J. *Makromol. Chem., Symp.* 1987, **10/11**, 331
31 Brandrup, J. and Immergut, E. H. 'Polymer Handbook', 3rd Edn., Wiley-Interscience, New York, 1989
32 van Doremaele, G. H. J. *PhD Thesis* Eindhoven University of Technology, 1990; van Doremaele, G. H. J., van Herk, A. M. and German, A. L. *Polym. Int.* in press
33 Matheson, M. S., Auer, E. E., Bevilacqua, E. B. and Hart, E. J. *J. Am. Chem. Soc.* 1951, **73**, 5395
34 van Doremaele, G. H. J., German, A. L., de Vries, N. K. and van der Velden, G. P. M. *Macromolecules* 1990, **23**, 4206
35 Buback, M., Garcia-Rubio, L. H., Gilbert, R. G., Napper, D. H., Guillot, J., Hamielec, A. E., Hill, D., O'Driscoll, K. F., Olaj, O. F., Shen, J., Solomon, D., Moad, G., Stickler, M., Tirrell, M. and Winnik, M. A. *J. Polym. Sci., Polym. Lett. Edn.* 1988, **26**, 293